



Zinc containing borate glasses and glass-ceramics: Search for biomedical applications

Amr M. Abdelghany^{1,*}, Fatema H. ElBatal², Hatem A. ElBatal²

¹*Spectroscopy Department, Physics Division, National Research Center, 12311, Cairo, Egypt*

²*Glass Research Department, National Research Center, 12311, Dokki, Cairo, Egypt*

Received 1 September 2014; Received in revised form 23 October 2014; Accepted 26 November 2014

Abstract

Ternary soda lime borate glass and samples with ZnO replacing CaO up to 10 mol% were prepared and studied for their bone bonding ability. Fourier transform infrared (FTIR) absorption spectra of the prepared glasses before and after immersion in simulated body fluid (SBF), for one or two weeks, showed the appearance of calcium phosphate (hydroxyapatite (HA)) which is an indication of bone bonding ability. X-ray diffraction patterns were measured for the glasses and indicated the presence of small peaks related to hydroxyapatite in the samples immersed in SBF. The glasses were heat treated with controlled two-step regime to convert them to their corresponding glass-ceramic derivatives. FTIR and X-ray diffraction measurements of the glass-ceramic samples (before and after immersion in SBF) confirmed the appearance of HA which is influenced by ZnO content. The overall data are explained on the basis of current views about the corrosion behaviour of borate glasses including hydrolysis and direct dissolution mechanism.

Keywords: glass-ceramics, $\text{Na}_2\text{O}\cdot\text{CaO}\cdot\text{B}_2\text{O}_3$ system, bioactivity, FTIR, XRD, SEM

I. Introduction

In recent years, many authors have been focused on the development of new materials that stimulate a biochemical response from living tissue in order to obtain a strong chemical bond with biological fixation between the prosthesis and the tissue [1,2]. Bioactive modified soda lime silica glass 45S5 (Bioglass[®]) is the oldest bioactive material, first reported by Hench *et al.* in 1971 [3] and is now a very well-characterized material that has found use in a number of biomedical applications such as orthopaedic implant and bone filling material [4].

Boron is the lightest element whose oxide can form glass alone or with plenty of other different oxides with diverse properties and applications. Glasses containing B_2O_3 have found applications such as fast ionic conductors, low temperature sealing devices, low-expansion scientific glassy equipment, radiation dosimetric devices, radioactive waste immobilization, biomaterials and as agriglass for plant nutrition [5–8].

Bioactivity or bone-bonding ability has been shown to depend on the chemical composition and structure of

bioactive glass [9,10]. In order to reach acceptable and improved bioactivity, incorporation of different oxides, such as MgO, ZnO or SrO, into various bioactive glasses has been investigated [11–14].

Zinc ions are assumed to play an important role in the growth of bone tissues in human body, although they are only present in trace amount [15]. Zinc ions have been known to encourage attachment, proliferation of osteoblasts and inhibit osteoclastic cells [16]. Moreover, zinc may serve as cofactor for many enzymes, stimulate protein synthesis responsible for DNA replication [17] and also involved in calcification mechanism [18]. It also inhibits the transformation of amorphous apatite into crystalline carbonated hydroxyapatite [19]. It is assumed that bioactive glass with high Zn content showed no apatite formation even after 60 days of immersion in simulated body fluid (SBF) [20].

In-vitro studies on some ZnO-containing silicate glasses have reached interesting results [20–25]. Thus, increasing the amount of Zn ions in silicate glass composition retards the dissolution process. This result is obviously due to the ability of ZnO to act as intermediate oxide (i.e. to act either as network former, ZnO_4 , or as modifier like alkali oxides and alkaline earth oxides). However, the increase of ZnO to high content

*Corresponding author: tel: +2 012211331525
fax: +2 02 33370931, e-mail: a.m_abdelghany@yahoo.com

showed no apatite formation, whereas the introduction of up to 10 mol% of ZnO is preferable and Fourier transform infrared (FTIR) measurements showed characteristic bands of hydroxyapatite [20–25]. In addition, borate based glasses (like phosphate-based glasses) represent special materials of measurable solubility in which the degradation profiles are predictable and can be controlled simply by carefully altering the chemical composition of the glasses.

The aim of this work was to study the effect of ZnO addition (replacing CaO up to 10 mol%) on the bioactivity of ternary soda lime borate glasses and their glass-ceramic derivatives by FTIR absorption spectral measurements after immersion of the glasses in SBF. The FTIR spectral studies were supplemented by scanning electron microscopic investigations of the glasses and glass-ceramics and X-ray diffraction analyses after immersion of the prepared samples in SBF for prolonged times.

II. Experimental details

2.1. Preparation of glass and glass-ceramics

Four different soda lime borate glasses with ZnO addition (Table 1) were prepared from accurately weighed batches by conventional melting and annealing technique. The raw materials include pure chemicals: orthoboric acid (H_3BO_3), Na_2CO_3 , $CaCO_3$ and ZnO. Melting was carried out in platinum crucibles in SiC heated furnace at 1100 °C for 2 hours. The crucibles were rotated to promote homogeneity to the melts. Then the melts were cast in preheated stainless steel molds of the appropriate dimensions. The glassy samples were immediately transferred to a muffle furnace regulated at 400 °C for annealing. After 1 hour the muffle was switched off and left to cool to room temperature at the rate of 30 °C/hour.

The parent glasses were thermally heat treated in two-step regime at temperatures determined by DTA measurement. Thus, each glass was slowly heated (5 °C/min) to the nucleation temperature (475 °C) insuring the formation of sufficient nuclei sites and after holding for the specified time (6 h), the samples were further heated to reach the second chosen crystal growth temperature (650 °C). Two letters (GC) were added in the notation of the obtained glass-ceramics to distinguish them from the parent glasses (i.e. Zn1 for the glass and ZnGC1 for the corresponding glass-ceramic).

2.2. Sample characterizations

The heat treated glasses were analysed by an X-ray diffraction (XRD) technique to identify the crystalline phases that were precipitated during the heat-treatment process. The heat-treated samples were grounded and the fine powder was examined using a Philips diffractometer (PW 1390) adopting a Ni-filter and a Cu-target. It should be mentioned that X-ray diffraction investigations were also carried out to characterize the glasses

and glass-ceramic samples before and after immersion in SBF at 37 °C for a period up to two weeks.

Fourier transform infrared (FTIR) absorption spectral measurements of the glasses and glass-ceramics were carried out through the KBr disc technique. The measurements were done at room temperature (~20 °C) in the wavenumber range of 4000–400 cm^{-1} using a Fourier transform IR spectrometer (Nicolet i10). Fine powders of the investigated samples were mixed with KBr powder in the ratio 1:100 and the mixtures were subjected to a load of 5 tons/ cm^2 in an evocable die to produce clear homogeneous discs. Then the FTIR spectra were immediately taken after preparing the discs to avoid moisture effect. The measurements were repeated after each immersion of the fine powders in simulated body fluid for prolonged times (1 or 2 weeks).

Scanning electron microscopic (SEM) investigations were carried out on the glass-ceramic derivatives before and after immersion in SBF for prolonged times. This study was performed using an SEM Model Philips XL 30, with attached EDX unit, using accelerating voltage of 30 kV. All samples were coated with gold for microstructural investigations.

Table 1. Chemical composition of the studied glasses

Glass	Na ₂ O [mol%]	CaO [mol%]	B ₂ O ₃ [mol%]	ZnO [mol%]
Zn1	15	25	60	0
Zn2	15	23	60	2
Zn3	15	20	60	5
Zn4	15	15	60	10

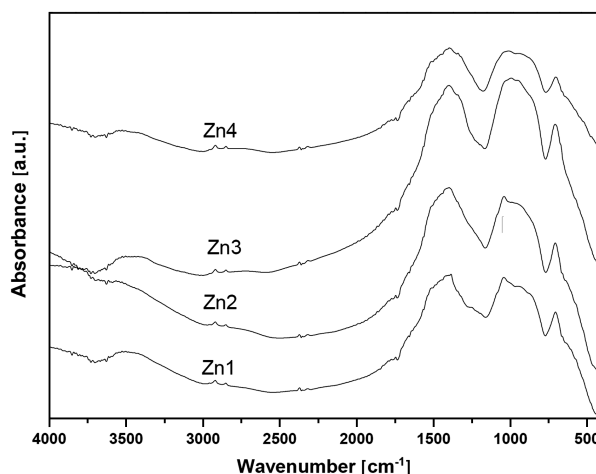


Figure 1. FTIR spectra of the studied glasses before immersion in SBF

III. Results

3.1. FTIR spectra of glasses before immersion in SBF

Figure 1 illustrates the FTIR absorption spectra of the studied glasses. The IR spectrum of the base ternary soda lime borate glass before immersion has the following characteristic features: i) a small peak at about 430

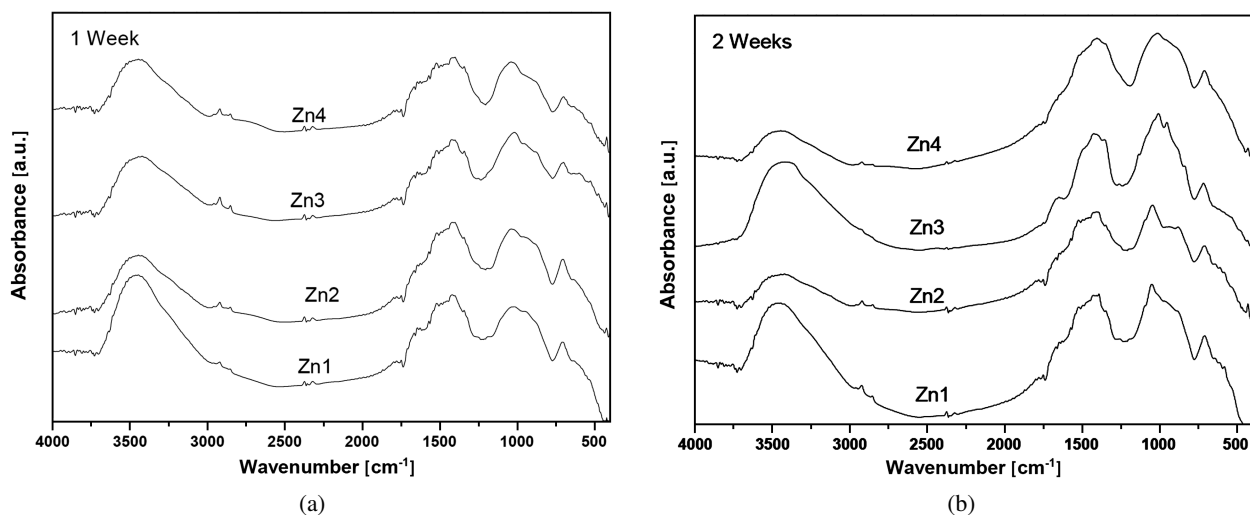


Figure 2. FTIR spectra of the studied glasses after immersion in SBF for: a) 1 and b) 2 weeks

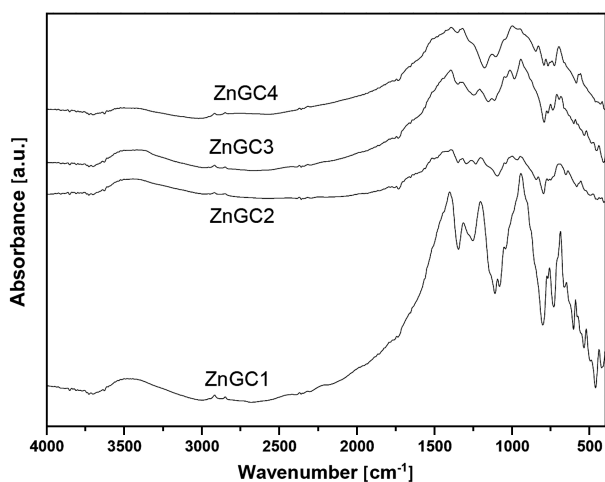


Figure 3. FTIR spectra of the studied glass-ceramics before immersion in SBF

cm⁻¹ followed by a kink at 490 cm⁻¹, ii) a small broad band with a peak at about 630 cm⁻¹, iii) distinct medium band with a peak at 712 cm⁻¹, iv) broad band extending from about 800 to 1200 cm⁻¹ (with three peaks at about 870, 940 and 1040 cm⁻¹), v) the second broad band extending from about 1250 to 1750 cm⁻¹ (with four peaks at about 1340, 1400, 1660 cm⁻¹), vi) four very small peaks at 2230, 2340, 2750 and 2830 cm⁻¹ and vii) medium broad band with a peak at 3460 cm⁻¹.

The glasses containing ZnO reveal FTIR spectra which are similar to the same vibrational bands identified in the ternary soda lime borate glass, and without any changes in the number and position of the IR vibrational bonds, while the two broad bands are somewhat broader.

3.2. FTIR spectra of glasses after immersion in SBF

Figure 2 reveals the FTIR absorption spectra of the glasses after immersion in SBF for 1 and 2 weeks. After one week of immersion the following IR spectral changes are observed: i) small peaks are identified

within the region from 450 to 650 cm⁻¹, ii) the second broad mid band from 1250 to 1750 cm⁻¹ is split to several small component peaks and iii) the near IR broad band at about 3460 cm⁻¹ becomes more intensified. After the immersion for two weeks in SBF, the FTIR spectra also exhibit the same changes observed after the immersion for one week.

3.3. FTIR spectra of glass-ceramics before immersion in SBF

Figure 3 illustrates the FTIR spectra of the glass-ceramic samples before immersion. The spectral data show two spectral details. The overall absorption bands within the mid region from 400 to 1650 cm⁻¹ reveal split sharp peaks for all the studied heat-treated samples and the first broad band is shifted and lies within the range from 1150–1550 cm⁻¹.

3.4. FTIR spectra of glass-ceramics after immersion in SBF

Figure 4 reveals the FTIR spectra of the glass-ceramic samples after immersion for one or two weeks. It is obvious that the IR spectra in Figs. 4a and 4b show almost the same spectral characteristics which indicate the splitting of the bands within the range from 400 to 1550 cm⁻¹ to numerous sharp peaks together with the increase of the intensity of the near IR broad band at 3460 cm⁻¹.

3.5. X-ray diffraction results

The investigations of the parent glasses by X-ray diffraction before immersion reveal no identified patterns in all studied samples as shown in Fig. 5. Upon immersion of the glassy samples in SBF, the X-ray diffraction results show small diffraction peaks increasing in intensity with the increase of ZnO content. These small peaks are related to hydroxyapatite.

Figure 6 illustrates the X-ray diffraction patterns of the glass-ceramic samples before immersion. The

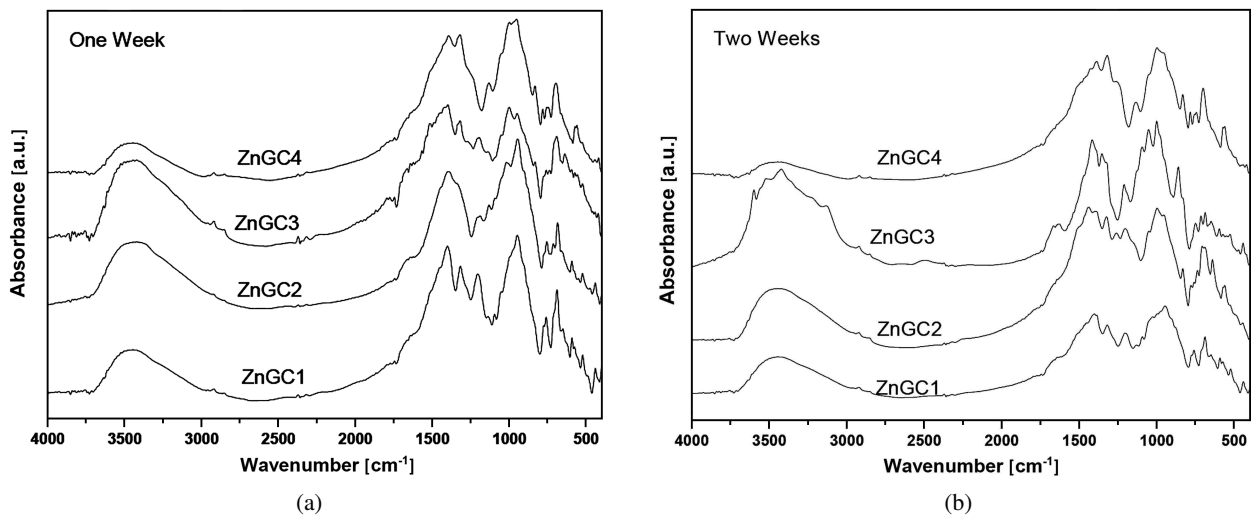


Figure 4. FTIR absorption spectra of the glass-ceramics after immersion in SBF for: a) 1 and b) 2 weeks

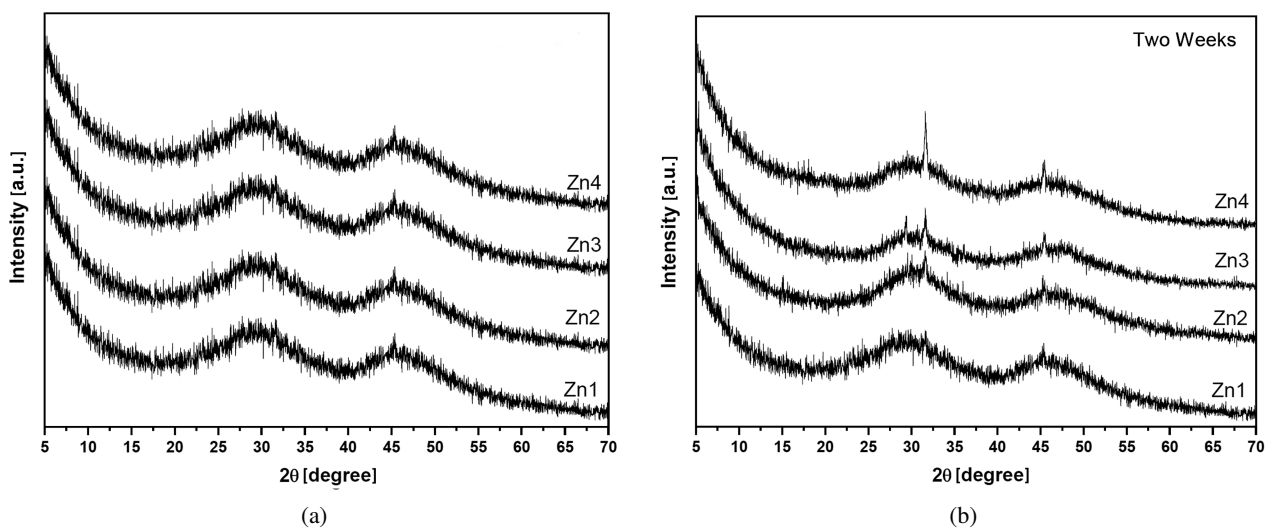


Figure 5. X-ray diffraction of the original glasses: a) before and b) after immersion in SBF for two week

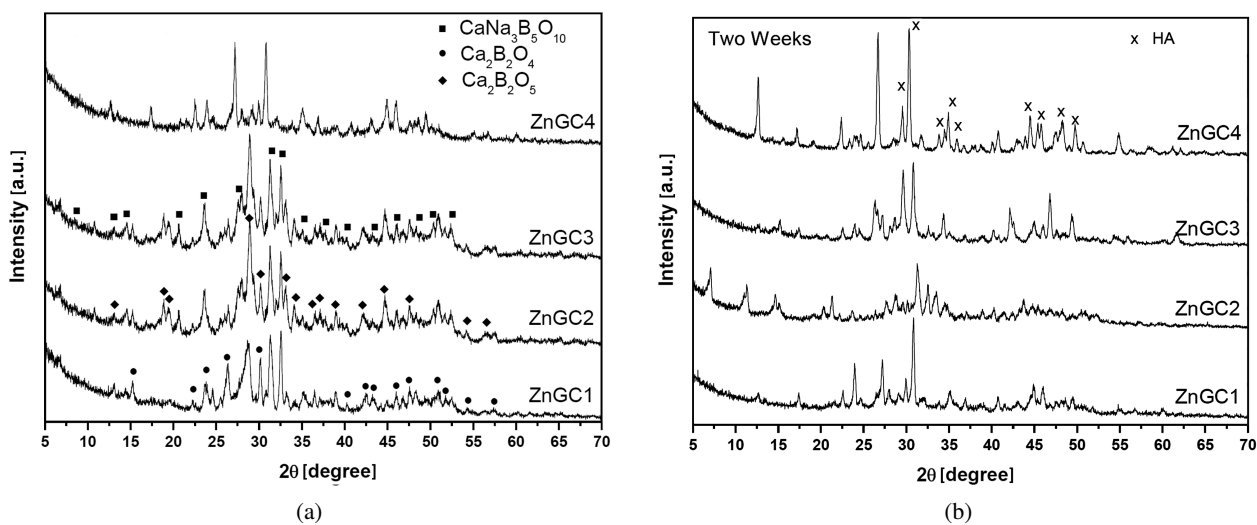


Figure 6. X-ray diffraction of the glass-ceramics before (a) and after immersion (b) in SBF for two week

crystalline phases identified are of crystalline calcium sodium borates and calcium borates. Upon immersion of the glass-ceramic samples for two weeks, the calcium borate phases are identified beside crystalline hydroxyapatite phase and this last HA phase increases in intensity with ZnO content.

3.6. Electron microscopic investigations

Figure 7 illustrates the SEM micrograph of the glass Zn1 before immersion. It is obvious that all glass samples before immersion show amorphous structure and no obvious effect of the increase of ZnO is noticed which is consistent with XRD data.

For all the studied glasses (Zn1→Zn4) upon immersion in SBF for two weeks, a needle like structure appears, representing the formation of precipitated microcrystals and the content of these needle crystals increases with increasing ZnO content as shown in Fig. 8.

Figure 9 illustrates the SEM micrographs of the glass-ceramics before and after immersion in SBF. The glass-ceramics before immersion have crystalline structure consisting of microsized crystals. The increase in size of the microcrystals is obvious with increasing ZnO

content (Fig. 9). After immersion in SBF, the glass-ceramics changes to a cotton-like structure indicating

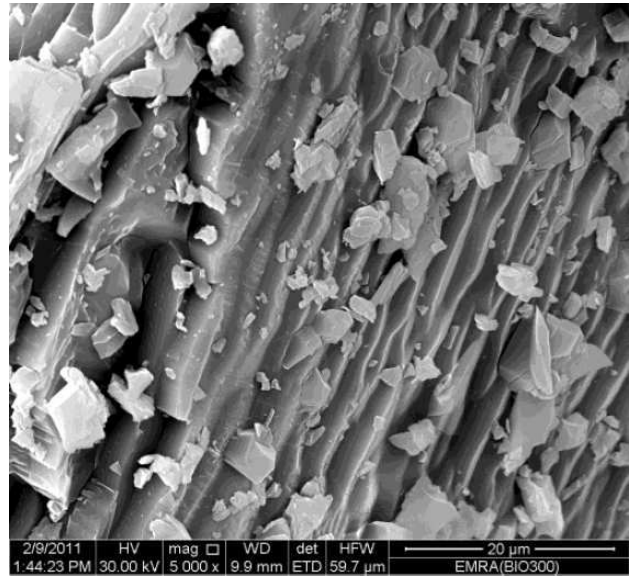
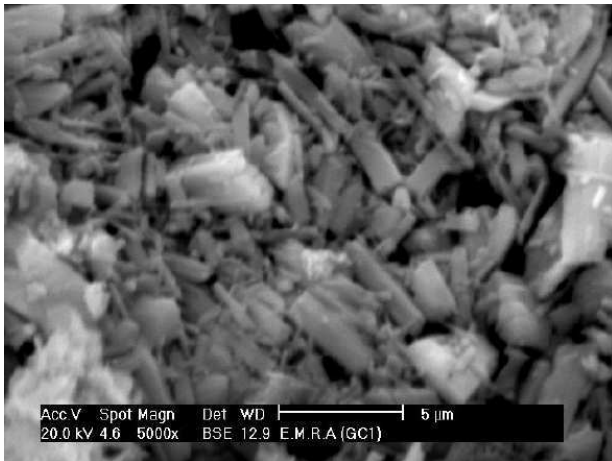
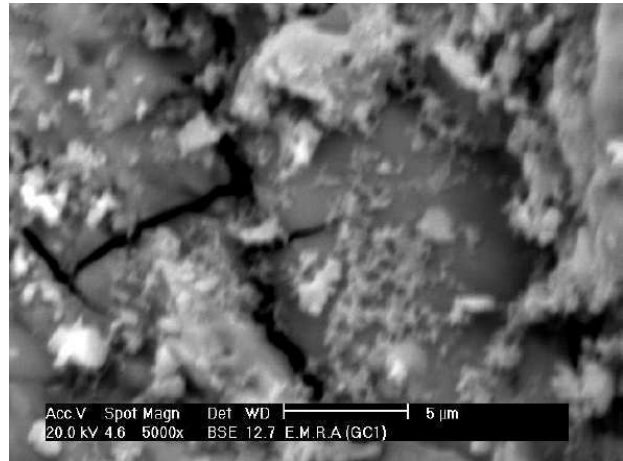


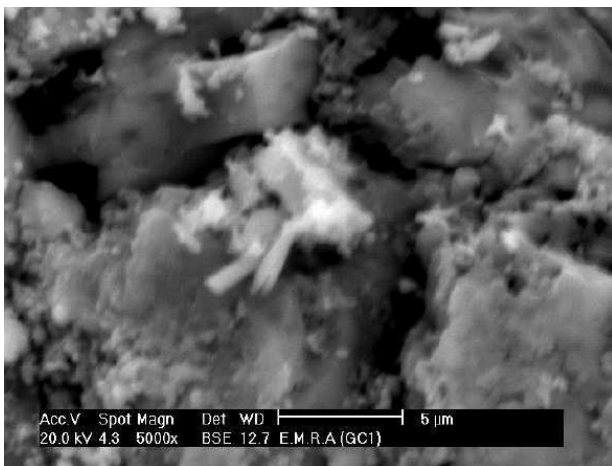
Figure 7. SEM image of the glass Zn1 before immersion



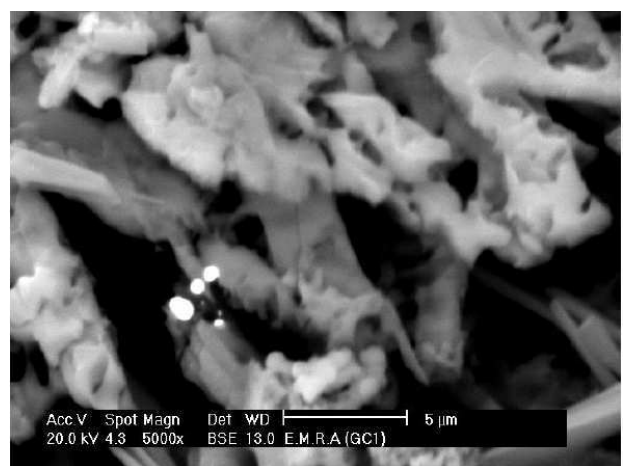
(a)



(b)



(c)



(d)

Figure 8. SEM images of the studied glasses after immersion in SBF for two weeks: a) Zn1, b) Zn2, c) Zn3 and d) Zn4

Table 2. The observed FTIR peaks and their assignment [28–31]

Peak position [cm ⁻¹]	Assignment
Borate groups	
B-O-B bending 690–700	Oxygen bridges between borons with 3- to 4-fold coordination or oxygen bridges between two borons with 3-fold coordination
BO4 group stretching	
850–900	Tri-, penta- and diborate groups vibrations
1020–1035	Tri-, penta-, tetra- and diborate vibrations
BO3 groups stretching	
1250	Tri-, penta- and tetraborate or boroxol vibrations
1400–1460	B–O vibrations of various borate groups
1500–1630	B–O bonds vibrations
Other vibrations	
2900–2925	Hydrogen bonding vibration
3430–3490	Vibration of molecular water
3740–3850	B–OH vibration
Metal ions	
400–450	Vibrations of Na ⁺ , Ca ²⁺ , Zn ²⁺

the appearance of crystalline phase which can be identified as calcium phosphate hydroxyapatite layer, what was already confirmed with XRD.

IV. Discussion

4.1. Interpretation of infrared spectra

Infrared spectroscopy is accepted to be a valuable and sensitive analytical method which needs only few milligrams to identify the detailed structural groups in various glasses in relation to their crystalline analogues [26,27]. This technique can be used for the confirmation of bioactivity in various bioglasses and bioglass-ceramics by the identification of hydroxyapatite layer or crystals after the immersion in SBF or phosphate solutions [8,28]. Also, IR spectral analyses are used to justify the mechanism of corrosion in glasses [29].

The studied borate glasses represent vitreous materials which possess rich chemistry. The basic boron element has the special ability to easily change its coordination with oxygen between three and four and hence can form variable units or groups with three or four coordinated boron atoms in glasses and crystalline derivatives [28–30]. Infrared spectra of borate glasses are identified from previous extended spectral studies to have the following characteristics [26,28–31]:

- The main vibrational modes associated with the borate network structure appear well above 500 cm⁻¹.
- The metal ions sites vibrational modes are mainly active in the far-IR region (below 500 cm⁻¹).
- The stretching tetrahedral borate unit (BO₄) vibrations are active in the region 800–1200 cm⁻¹.
- The stretching trigonal borate unit (BO₃ or BO₂O) vibrations are active in the wavenumber range of 1200–1500 cm⁻¹.
- The bending vibrations of various borate groups are active at 600–800 cm⁻¹.

Based on these previous considerations, it can be stated that the identification and separations of differently coordinated borate groups are to be carried out with marked accuracy with their different vibrational wavenumbers. The interpretations of the IR spectra of the studied borate glasses before immersion are summarized in Table 2.

The appearance of vibrational modes due to both triangular and tetrahedral borates with comparable intensities can be realized and explained as follows:

- The presence of both alkali oxide (Na₂O) and alkaline earth oxide (CaO) in the studied base glasses causes some of the borons in B₂O₃ to change from triangular to tetrahedral coordination while nonbridging oxygen is not formed at the beginning.
- The conversion of borons from 3- to 4-fold coordination ceases when the concentration of tetrahedrally coordinated borons reaches some critical concentration and after which any additional modifier oxide causes the formation of nonbridging oxygen.
- The combined strong presence of both vibrational bands due to triangular borate units at 1250–1600 cm⁻¹ and tetrahedral borate units at 800–1200 cm⁻¹ confirms the previous suggestions that the tetrahedral borate units are generated by the action of both Na₂O and CaO.

4.2. Effect of immersion in SBF on FTIR spectra

Experimental FTIR results (Fig. 2) indicate two important changes upon the immersion of the glasses in SBF for one or two weeks: i) the appearance of small peaks within the wavenumber range 500–650 cm⁻¹ (which become more intense with longer immersion time) and ii) the decrease of vibrational modes intensity due to BO₃ groups in the range of 1250–1650 cm⁻¹. The presence of these peaks is attributed to the formation of calcium phosphate (hydroxyapatite)

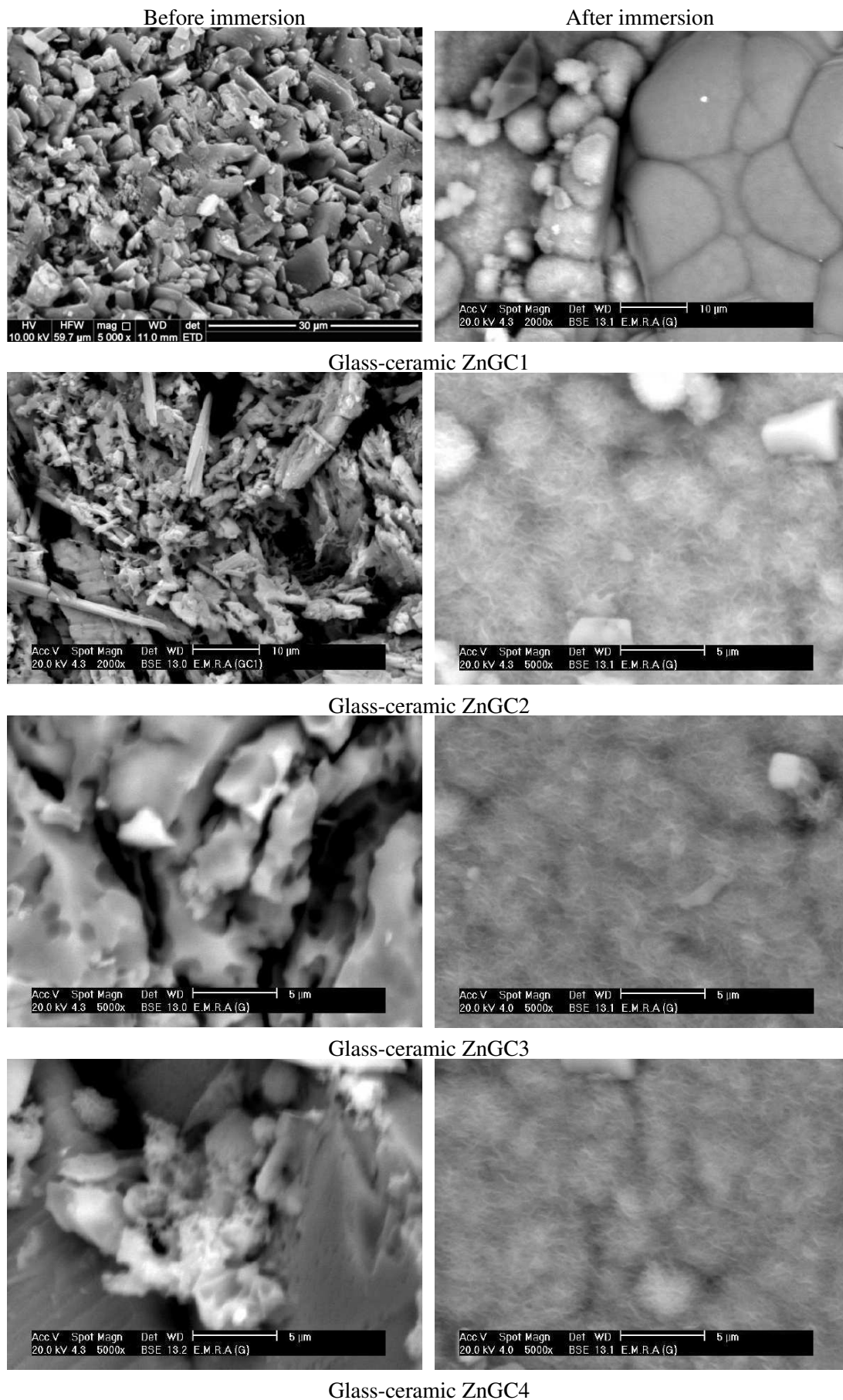


Figure 9. SEM images for the prepared glass-ceramics before (left) and after immersion (right) in SBF for two weeks

and the decrease in amount of the borate phase with triangular coordination. It is assumed that the borate phase with triangular coordination dissolves in the immersion fluid faster than the tetrahedrally coordinated borate phase. This is due to the fact that BO_4 units are attached firmly to four equal directions beside the firm linking of alkali or alkaline earth cation to achieve neutrality while the BO_3 units are attached to three directions.

FTIR spectra of the glass-ceramics (Fig. 3) reveal distinct numerous sharp peaks all over the characteristic wavenumbers for both BO_3 and BO_4 vibrations. After immersion, the distinct peaks due to hydroxyapatite at (at $500\text{--}650\text{ cm}^{-1}$) are clearly identified when the time of immersion was extended to two weeks.

4.3. Effect of ZnO addition on FTIR spectra

Careful inspection of the FTIR data of the glasses and their glass-ceramic derivatives before and after immersion in SBF indicates that the successive increase of ZnO replacing CaO did not change the presence of vibrational bands due to tetrahedral borate units in comparison to the bands due to trigonal borate units. This indicates that ZnO behaves like CaO and Na_2O in the promotion of the conversion process of some BO_3 to BO_4 groups or some of ZnO act as ZnO_4 forming units. In addition, the FTIR spectra of the glasses after immersion for one or two weeks indicate that the vibrational bands are stable in position and also in intensity. This implies that ZnO causes the chemical stability of the glasses and their resistance to rapid dissolution expected for alkali or alkaline borate glasses. Several glass scientists [24,25] have assumed that ZnO can exist either as a network forming ZnO_4 tetrahedra or as in octahedral modifying positions. Such ability to form structural units can attribute the increase of chemical durability when ZnO replaces CaO.

4.4. Interpretation of XRD data

Experimental XRD data indicate the separation of crystalline phases upon controlled thermal heat treatment of the studied borate glasses (Fig. 6a). It has been recognized that the type of the formed microcrystalline phases depends on the composition and constituent of the glasses and on heat treatment condition [32]. It is obvious that all the phases identified from the crystallization of borate glasses contain calcium sodium borate ($2\text{CaO}\cdot 3\text{Na}_2\text{O}\cdot 5\text{B}_2\text{O}_3$) and two different types of crystalline calcium borate ($2\text{CaO}\cdot \text{B}_2\text{O}_3$ and $\text{CaO}\cdot \text{B}_2\text{O}_3$) with different ratios depending on the glass constituents. These results can be realized and interpreted on the basis of the assumption of Hudon and Baker [33] for the readiness of calcium ions (Ca^{2+}) to initiate the nucleation and crystallization of glasses. A cotton-like structure, obtained after immersion of the glass-ceramics in SBF, indicates the appearance of hydroxyapatite layer.

Zinc ions (Zn^{2+}) are assumed to act in glass both as weak tetrahedral network former and as modifier cations [34–37]. With the increase of ZnO replacing CaO, the

amount of available nonbridging oxygen (assists in formation of ZnO_4 group) decreases. It is assumed that Zn^{2+} ions are situated in modifier positions and with this the chemical stability is reached without further formation of ZnO_4 groups.

V. Conclusions

Soda lime borate glasses containing 2–10 mol% ZnO substituting CaO were prepared and characterized for their bone bonding ability after immersion in SBF up to two weeks. FTIR spectra reveal the appearance of two characteristic bands within the wavenumber range from $530\text{--}650\text{ cm}^{-1}$ indicating the formation of hydroxyapatite. The glasses were thermally treated to their corresponding glass-ceramic derivatives producing crystalline calcium sodium borate and different forms of calcium borate phases. The immersion of these glass-ceramics into SBF for two weeks produces crystalline hydroxyapatite.

Scanning electron microscopic investigations of the prepared glasses reveal amorphous nature of the glasses which after immersion indicates some features of hydroxyapatite. The glass-ceramics show the morphological features of micro-crystalline calcium sodium borate and calcium borate before immersion. After immersion, the rounded crystalline features of hydroxyapatite are identified and increases with the ZnO content.

References

1. W. Liang, M.N. Rahaman, D.E. Day, N.W. Marion, G.C. Riley, J.J. Mao, "Bioactive borate glass scaffold for bone tissue engineering", *J. Non-Cryst. Solids*, **354** (2008) 1690–1696.
2. C.R. Mariappan, D.M. Yunos, A.R. Boccaccini, B. Roling, "Bioactivity of electro-thermally poled bioactive silicate glass", *Acta Biomater.*, **5** [4] (2009) 1274–1283.
3. L.L. Hench, R.J. Splinter, W.C. Allen, T.K. Greenlee, "Bonding mechanisms at the interface of ceramic prosthetic materials", *J. Biomed. Mater. Res.*, **5** [6] (1972) 117–141.
4. W. Cao, L.L. Hench, "Bioactive materials", *Ceram. Int.*, **22** [6] (1996) 493–507.
5. L.L. Hench, "Bioceramics, a clinical success", *J. Am. Ceram. Soc.*, **81** [7] (1998) 1705–1727.
6. F.M. EzzEldin, "Leaching and mechanical properties of cabal glasses developed as matrices for immobilization high-level wastes", *Nucl. Instr. Meth. Phys. Res. B.*, **183** [3-4] (2001) 285–300.
7. A.M. Abdelghany, H.A. ElBatal, L. Mari, "Optical and shielding behavior studies of vanadium doped lead borate glasses", *Radiat. Eff. Defect Solids*, **167** [1] (2012) 49–58.
8. A.M. Abdelghany, H.A. ElBatal, F.M. EzzEldin, "Bone bonding ability behavior of some ternary borate glasses by immersion in sodium phosphate solution", *Ceram. Int.*, **38** (2012) 1105–1113.

9. R.G. Hill, D.S. Brauer, “Predicting the bioactivity of glasses using the network connectivity or split network models”, *J. Non-Cryst. Solids*, **357** (2011) 3884–3887.
10. M.D. O’Donnel, R.G. Hill, “Influence of strontium and the importance of glass chemistry and structure when designing bioactive glasses for bone regeneration”, *Acta Biomater.*, **6** (2010) 2382–2385.
11. J. Ma, C.Z. Chen, D.G. Wang, J.H. Hu, “Low-temperature sintering and microwave dielectric properties of 3Z2B glass–Al₂O₃ composites”, *Ceram. Int.*, **37** (2011) 2377–2382.
12. A.M. AlKady, A.F. Ali, “Fabrication and characterization of ZnO modified bioactive glass nanoparticles”, *Ceram. Int.*, **38** (2012) 1195–1204.
13. X. Wang, X. Li, A. Ito, Y. Sogo, “Synthesis and characterization of hierarchically macroporous and mesoporous CaO–MO–SiO₂–P₂O₅ (M = Mg, Zn, Sr) bioactive glass scaffolds”, *Acta Biomater.*, **7** (2011) 3638–3644.
14. M. Yamaguchi, H. Oishi, Y. Suketa, “Stimulatory effect of zinc on bone formation in tissue culture”, *Biochem. Pharmacol.*, **36** (1987) 4007–4012.
15. K. Ishikawa, Y. Miyamomoto, T. Yuasa, A. Ito, M. Nagayama, K. Suzuki, “Fabrication of Zn containing apatite cement and its initial evaluation using human osteoblastic cells”, *Biomater.*, **23** (2002) 423–428.
16. Y.F. Goh, A.Z. Alshemary, M. Akram, M.R. Abdul Kadir, R. Hussain, “In vitro study of nano-sized zinc doped bioactive glass”, *Mater. Chem. Phys.*, **137** [3] (2013) 1031–1038.
17. M. Yamaguchi, K. Inamoto, Y. Suketa, “Effect of essential trace metals on bone metabolism in weanling rats: Comparison with zinc and other metals’ actions”, *Res. Exp. Med.*, **186** [5] (1986) 337–342.
18. R.L. Du, J. Chang, “Preparation and characterization of Zn and Mg doped bioactive glasses”, *J. Inorg. Mater.*, **19** [6] (2004) 1353–1358.
19. J.R. Jaroch, D.C. Clupper, “Modulation of zinc release from bioactive sol-gel SiO₂–CaO–ZnO glasses and ceramics”, *J. Biomed. Mater. Res. A.*, **82** (2007) 575–588.
20. G. Lusvardi, G. Malavasi, L. Menabue, M.C. Menziani, “Synthesis, characterization, and molecular dynamics simulation of Na₂O–CaO–SiO₂–ZnO glasses”, *J. Phys. Chem. B*, **106** (2002) 9753–9760.
21. L. Linanti, G. Lusvardi, G. Manabue, M.C. Menziani, A. Pedone, U. Segre, V. Aina, A. Perardi, M. Cannas, “Properties of zinc releasing surfaces for clinical applications”, *J. Biomater. Appl.*, **22** (2008) 505–526.
22. V. Aina, G. Malavasi, A. Fiorio Pla, L. Munaron, C. Moretena, “Zinc-containing bioactive glasses: Surface reactivity and behaviour towards endothelial cells”, *Acta Biomater.*, **5** (2009) 1211–1222.
23. S. Haimi, G. Gorianc, L. Moimas, B. Lindroos, H. Huhtala, S. Raty, H. Kuokkanen, G.K. Sandor, C. Schmid, S. Miettinen, R. Suuronen, “Characterization of zinc-releasing three-dimensional bioactive glass scaffolds and their effect on human adipose stem cell proliferation and osteogenic differentiation”, *Acta Biomater.*, **5** [8] (2009) 3122–3131.
24. J.C. Hurt, C.J. Philips, “An investigation of the effects of zinc oxide on the structure of glasses in the system Na₂O–ZnO–SiO₂”, *J. Am. Ceram. Soc.*, **53** (1971) 269–273.
25. A.B. Rosenthal, S.H. Garofalini, “Structural role of zinc oxide in silica and soda-silica glasses”, *J. Am. Ceram. Soc.*, **70** (1987) 821–826.
26. J. Wong, C.A. Angell, *Glass Structure by Spectroscopy*, Marcel Dekker, New York, 1977.
27. S-B. Cho, K. Nakanishi, T. Koukubo, N. Soga, C. Ohtsuki, T. Nakamura, T. Kitsugi, T. Yamamuro, “Dependence of apatite formation on silica gel on its structure: Effect of heat treatment”, *J. Am. Ceram. Soc.*, **78** (1995) 1769–1774.
28. M.A. Ouis, A.M. Abdelghany, H.A. ElBatal, “Corrosion mechanism and bioactivity of borate glasses analogue to Hench’s bioglass”, *Process. Appl. Ceram.*, **6** [3] (2012) 141–149.
29. F.H. Margha, A.M. Abdelghany, “Bone bonding ability of some borate bio-glasses and their corresponding glass-ceramic derivatives”, *Process. Appl. Ceram.*, **6** [4] (2012) 183–192.
30. E.I. Kamitsos, A. Patsis, M.A. Karkassides, G.D. Chryssikos, “Infrared reflectance spectra of lithium borate glasses”, *J. Non-Cryst. Solids*, **126** (1990) 52–67.
31. E.I. Kamitsos, “Infrared studies of borate glasses”, *Phys. Chem. Glasses*, **44** (2003) 79–87.
32. W. Holland, G. Bell, *Glass Ceramic Technology*, The American Ceramic Society, Westerville, OH, USA, 2002.
33. P. Hudon, D.R. Baker, “The nature of phase separation in binary oxide melts and glasses. I. Silicate systems”, *J. Non-Cryst. Solids*, **303** [3] (2002) 299–345.
34. M.A. Azooz, S.A.M. Abdel-Hameed, “Synthesis, characterization and magnetic properties of glass ceramics containing nanoparticles of both Ba-hexaferrite and Zn-ferrite”, *Ceram. Int.*, **40** [3] (2014) 4499–4505.
35. G. Lusvardi, G. Malavasi, L. Menabue, M.C. Menziani, U. Segre, M.M. Carnasciali, A. Ubaldini, “A combined experimental and computational approach to (Na₂O)_{1-x}·CaO·(ZnO)_x·2 SiO₂ glasses characterization”, *J. Non-Cryst. Solids*, **345** (2004) 710–714.
36. G. Ennas, A. Musinu, G. Piccaluga, A. Montenero, G. Gnappè, “Structure and chemical durability of zinc-containing glasses”, *J. Non-Cryst. Solids*, **125** (1990) 181–185.
37. A.A. Khedr H.A. ElBatal, “Corrosion of zinc-containing cabal glasses by various leaching solutions”, *J. Am. Ceram. Soc.*, **79** [3] (1996) 733–741.

